

## Optical anisotropy of (113)-oriented GaAs/AlAs superlattices

G. Armelles, P. Castrillo, P. S. Dominguez, L. González, and A. Ruiz

*Centro Nacional de Microelectrónica, Consejo Superior de Investigaciones Científicas, Serrano 144, 28006 Madrid, Spain*

D. A. Contreras-Solorio,\* V. R. Velasco, and F. García-Moliner

*Instituto de Ciencia de Materiales, Consejo Superior de Investigaciones Científicas, Serrano 123, 28006 Madrid, Spain*

(Received 31 August 1993; revised manuscript received 21 December 1993)

The optical properties of (113)-oriented GaAs/AlAs superlattices grown by atomic-layer molecular-beam epitaxy at low substrate temperature have been studied by means of piezoreflectance techniques. Several transitions have been detected which exhibit heavy-hole and light-hole character. The heavy-hole transitions are more polarized along the  $[3\bar{3}2]$  direction whereas the light-hole transitions are more polarized along the  $[1\bar{1}0]$  direction. We have also performed calculations for these superlattices by using an empirical tight-binding Hamiltonian. According to the results thus obtained the observed optical anisotropy is related to the different components of the valence-band wave functions of the superlattices.

The optical properties of semiconductor quantum wells (QW's) and superlattices (SL's) are strongly dependent on the growth direction. For example, the photoluminescence intensity of (111)-oriented GaAs/Al<sub>x</sub>Ga<sub>1-x</sub>As quantum wells is greater than that of (001)-oriented systems.<sup>1</sup> This fact has been attributed to the heavier mass of the heavy-hole band in GaAs along the  $[111]$  direction compared to the  $[001]$  direction; such a difference gives rise to a larger density of states.<sup>1</sup> Moreover, if the heterostructures are grown on substrates with orientations different from (001) or (111) one may expect the appearance of in-plane optical anisotropies, as it has been observed in (110)-oriented GaAs/Al<sub>x</sub>Ga<sub>1-x</sub>As quantum wells.<sup>2</sup>

In some cases the properties of the systems are also dependent on the growth method: (113)-oriented GaAs/AlAs superlattices grown by conventional molecular-beam epitaxy (MBE) have a corrugated interface which gives rise to a quantum-wire-like structure.<sup>3,4</sup> Such corrugation is not present if the heterostructures are grown by atomic layer molecular-beam epitaxy (ALMBE).<sup>5</sup>

GaAs/AlAs superlattices grown by MBE present in-plane optical anisotropies, which were attributed to the quantum-wire-like structures present in those samples.<sup>3,4</sup> Our aim is to study the in-plane optical anisotropy in noncorrugated superlattices, grown by ALMBE, and establish whether the anisotropy observed in corrugated superlattices is really linked to the quantum-wire structure or if it is related to an intrinsic property of (113)-oriented heterostructures. For that purpose we have performed piezoreflectance measurements. The sample was thinned to 150  $\mu\text{m}$  and glued into a piezoelectric transducer. The transducer was driven by a sinusoidal electric field. That field produces a sinusoidal strain in the (113) plane. The magnitude of this strain is very small ( $\epsilon_{ij} \leq 10^{-5}$ ) which implies that the coupling induced by this strain between the different levels of the superlattice is negligible. The principal effect of the modulated strain applied to the samples is to modulate the energy position

of the transitions. The piezoreflectance spectra thus obtained are similar to the wavelength modulated spectra,<sup>6</sup> the difference being the magnitude of the energy modulation which depends on the type of the transition. In particular, the light-hole (lh) transitions are enhanced in the piezoreflectance spectra compared to the wavelength modulated spectra.<sup>7</sup> In our experimental setup the sample was illuminated with light polarized parallel to  $[1\bar{1}0]$  or  $[3\bar{3}2]$  and the reflected light was analyzed by a monochromator of 300 cm of local length and detected by a Si photodiode. The signal of the photodiode has two components, one proportional to the reflectance (dc component) and the other proportional to the modulated reflectance which was measured using a lock-in amplifier tuned to the modulated frequency. Both signals, the dc component of the photodiode and the output of the lock-in amplifier, were recorded by a computer to obtain the normalized change in reflectance  $\Delta R/R$ . The experimental results are compared with calculations based on an empirical tight-binding (ETB) Hamiltonian.<sup>8</sup> The optical anisotropies observed for these (113) GaAs/AlAs superlattices are related to the different components of the valence-band wave function levels.

In Fig. 1 we present the piezoreflectivity spectra of the samples studied here, (AlAs)<sub>74</sub>(GaAs)<sub>17</sub> and (AlAs)<sub>58</sub>(GaAs)<sub>8</sub>, where the subindexes are expressed in monolayers, for the two in-plane polarizations  $[1\bar{1}0]$  and  $[3\bar{3}2]$ .

Together with a small sinusoidal component related to the piezomodulation of the thickness of the epilayer, which gives rise to damped Fabry-Pérot oscillations, we observe several transitions. They are located at 1.8 eV, 1.88 eV, and 2.15 eV in sample 1 and at 2.02 eV, 2.12 eV and 2.39 eV in sample 2. We label these transitions as heavy-hole- (hh) like, light-hole-like, and spin-orbit- (s.o.) like, respectively. Such labeling is made according to the different polarization properties and will be discussed later.

As the GaAs well thickness is decreased there is an increase in the relative intensity of the hh-like and s.o.-like

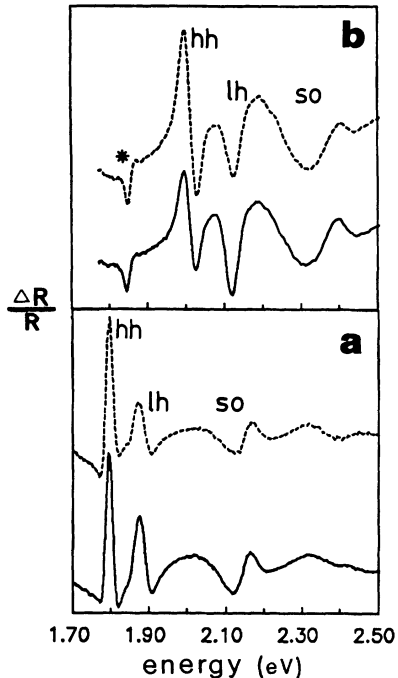


FIG. 1. Piezoreflectance spectra of the (a)  $(\text{AlAs})_{74}(\text{GaAs})_{17}$  and (b)  $(\text{AlAs})_{58}(\text{GaAs})_8$  superlattices obtained at 80 K. Solid line: light polarized parallel to  $[1\bar{1}0]$ . Dashed line: light polarized parallel to  $[33\bar{2}]$ . The s.o. transition of the GaAs substrate is also observed in sample (b) (\*).

features of the  $[33\bar{2}]$  spectrum as compared to the  $[1\bar{1}0]$  spectrum. The opposite happens for the lh-like feature. In Table I we present the relative intensity of the different transitions observed in the spectra of Fig. 1.

In order to understand these results we have performed calculations with an ETB Hamiltonian with an  $sp^3s^*$  orbital basis,<sup>8</sup> and interactions up to nearest neighbors only, including spin-orbit splitting<sup>9</sup> together with the surface Green function matching (SGFM) method.<sup>10</sup> This approach gave good results for the case of the (001) superlattices<sup>11,12</sup> and can be easily applied to the case of (113) superlattices and quantum wells.<sup>13</sup> In this case the ETB Hamiltonian must be transformed to the new axes corresponding to the (113) interfaces. All the details concerning the empirical matrix elements used in this calculation, the interface interactions, and the formal aspects of the calculation can be found in Ref. [13] and need not be repeated here.

We have assumed that the valence-band offset of lattice matched GaAs/AlAs heterostructures is not direction dependent<sup>14</sup> and we have used the same values of

TABLE I. Experimental and theoretical intensity ratios of the different transitions observed.

$I_{[1\bar{1}0]}/I_{[33\bar{2}]}$	$(\text{AlAs})_{74}(\text{GaAs})_{17}$		$(\text{AlAs})_{58}(\text{GaAs})_8$	
	Expt.	Theory	Expt.	Theory
hh	0.9	0.86	0.7	0.77
lh	1.4	1.22	1.5	1.36
s.o.	1.2	1.04	1.0	0.94

the (001) heterostructures. Some calculations indicate a small variation of the band offset with the different orientations.<sup>15,16</sup> We have made some calculations allowing for these variations in the band offset and we have found only small shifts (some meV) in the positions of some states, but without modifying the overall picture extracted with the unmodified band offset. The effective masses of the conduction electron, and light holes in the  $[113]$  directions coming from our bulk ETB Hamiltonian are higher than those obtained by other means.<sup>17</sup> This can introduce some error in the numerical values of the corresponding transitions, but without altering the qualitative picture.

Due to the lower symmetry of the (113)-oriented heterostructures, as compared with the (001)-oriented ones, the envelope wave function of the different levels has no well defined parity, as can be observed in Fig. 2, where we present the spatial distribution of the spectral strength<sup>10</sup> for the first conduction level with a strong  $s$  component and the two first valence levels, for the two samples studied here. In spite of this, it is useful to employ the same nomenclature of the (001)-oriented superlattices for the confined levels of these two structures. The  $n = 1$  levels have no nodes, the  $n = 2$  have one node around the middle of the GaAs well, etc. According to our calculations, sample 1 has six levels in the valence band which are localized in the GaAs layers and correspond to the  $n = 1 - 3$  hh-like levels,  $n = 1 - 2$  lh-like levels, and  $n = 1$  s.o.-like level. The character of the valence levels is established by the relative intensity of the  $p_x$ ,  $p_y$ , and  $p_z$  components.

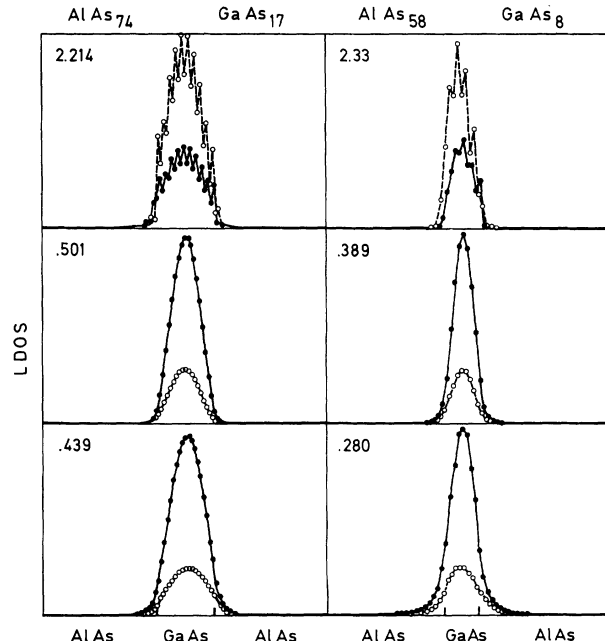


FIG. 2. Spatial distribution of the total spectral strength local density of states (LDOS) for the levels discussed in the text. The  $\bullet$  corresponds to the anion layers and the  $\circ$  to the cation layers. The energy position (in eV) of the levels is also given.

The  $p_y$  component of the hh-like levels is greater than the  $p_x$  component and these levels have very small  $p_z$ ,  $s$  and  $s^*$ , components. On the other hand, the  $p_x$  component of the lh-like levels is greater than the  $p_y$  and all have a  $p_z$  component which in some cases is greater than the other two [remember that for (001)-oriented SL's the hh-like levels have a negligible  $p_z$  component and equal  $p_x$  and  $p_y$  components, whereas the lh-like levels have a strong  $p_z$  component and also equal  $p_x$  and  $p_y$  components]. The other sample presents four valence levels with strong spectral strength in the GaAs layers; two of them also have non-negligible spectral strength in the AlAs layers. The character of the most confined levels is clearly hh-like and lh-like, with the  $p_y$  component greater than the  $p_x$  one in the hh-like level. This ordering is reversed in the lh-like level and the  $p_z$  component here is greater than the other two. The character of the other two levels is not so well defined. As an example we present in Fig. 3 the spatial distribution of the  $p_x$  and  $p_y$  contributions to the spectral strength for the first hh and lh levels of the two samples. For the sake of clarity only the anion layers have been presented.

There are several conduction levels having a strong spectral strength in the GaAs layers, but only a few of them have a strong  $s$  component.

We interpret the observed transitions, labeled as hh and lh, as arising between the first hh and lh states (located in sample 1 at 0.501 eV and 0.439 eV, respectively, and in sample 2 at 0.389 eV and 0.280 eV, respectively) and the first conduction states with a strong  $s$  component (located in sample 1 at 2.214 eV and in sample 2 at 2.33 eV). The transition labeled s.o. originates from the valence state at 0.132 eV and the conduction state at 2.214 eV in sample 1, and from the valence state at 0.046 eV or 0.018 eV and the conduction state at 2.33 eV in sample 2.

The origin of the different contributions of the  $p_x$  and  $p_y$  components to the valence-band states of the SL's is

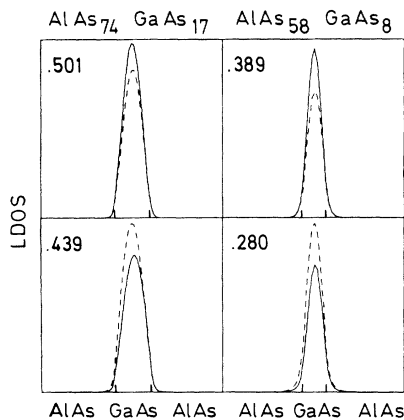


FIG. 3. Envelope of the spatial distribution of the contributions to the total spectral strength of the  $p_x$  component (dashed line) and  $p_y$  component (solid line) for the first hh level [located at 0.501 eV in the  $(\text{AlAs})_{74}(\text{GaAs})_{17}$  SL and at 0.389 eV in the  $(\text{AlAs})_{58}(\text{GaAs})_8$  SL, respectively] and the first lh level [located at 0.439 eV in the  $(\text{AlAs})_{74}(\text{GaAs})_{17}$  SL and at 0.280 eV in the  $(\text{AlAs})_{58}(\text{GaAs})_8$  SL, respectively].

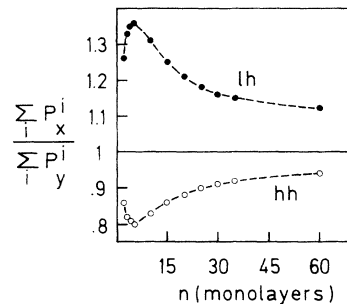


FIG. 4. Ratio of the integrated  $p_x$  and  $p_y$  components as a function of the QW thickness (in monolayers) for the first hh-like and lh-like states, in a GaAs/AlAs quantum well.

based on the low symmetry of the [113] direction. [001] and [111] are high symmetry directions and the wave functions of the heavy-hole band and light-hole band of bulk material along these directions have equal in-plane components [ $p_x=p_y$  with  $x$  and  $y$  in the (001) or (111) plane]. As a consequence no in-plane anisotropy is expected in the heterostructures (QW or SL) grown on those planes, but for the [113] direction this is not true and then in-plane anisotropies may appear in the heterostructures grown on this plane.

To have an idea of the theoretical optical anisotropy of the different transitions we have performed a calculation where the intensity of the optical transition is proportional to the overlap of the  $p_x$  ([110] spectra) and  $p_y$  ([332] spectra) components of the valence-band wave function and the  $s$  component of the conduction-band wave function. In this calculation we neglect the matrix elements between nearest neighbors, which is not a bad approximation due to the difference between its value and that of the intra-atomic transitions. The results of this calculation are presented in Table I, and it can be observed that the agreement with the experiment is quite good. We have assumed that the dipolar matrix elements of the As atoms is three times that of the Ga or Al atoms.<sup>18</sup> Similar results are obtained using other relations.

The degree of optical anisotropy depends on the transition and on the composition of the SL. As an example we present in Fig. 4 the ratio of the integrated  $p_x$  and  $p_y$  components as a function of the QW thickness for the first hh-like and lh-like states, in a GaAs/AlAs QW. This ratio gives an idea of the in-plane optical anisotropy of a transition. A value equal to 1 means no in-plane anisotropy.

We would like to point out that the observed optical anisotropy is not related to any kind of quantum-wire structure, not present in our samples, but to the different components of the valence-band wave functions. Moreover, the optical anisotropy observed in samples with quantum-wire-like structure are of the same order as those found here, which may imply that the corrugation has a small effect on the observed anisotropies.

This work was partially supported by the Comisión Interministerial de Ciencia y Tecnología, under Grants No. MAT91-0738 and No. MAT92-0262. One of us (D.A.C.-S.) is grateful to the European Community for support.

- \* Permanent address: Escuela de Física, Universidad Autónoma de Zacatecas, Apdo. Postal C-580, 98068 Zacatecas, Zac., Mexico.
- <sup>1</sup> T. Hayakawa, K. Takahashi, M. Kondo, T. Suyama, S. Yamamoto, and T. Hijikata, *Phys. Rev. Lett.* **60**, 349 (1988).
- <sup>2</sup> D. Gershoni, I. Brener, G. A. Baraff, S. N. G. Chu, L. N. Pfeiffer, and K. West, *Phys. Rev. B* **44**, 1930 (1991).
- <sup>3</sup> R. Nötzel, N. N. Ledentsov, L. Däweritz, H. Hohenstein, and K. Ploog, *Phys. Rev. Lett.* **67**, 3812 (1991).
- <sup>4</sup> R. Nötzel, N. N. Ledentsov, L. Däweritz, K. Ploog, and M. Hohenstein, *Phys. Rev. B* **45**, 3507 (1992).
- <sup>5</sup> F. Briones, L. González, and A. Ruiz, *Appl. Phys. A* **49**, 729 (1989).
- <sup>6</sup> P. Castrillo, M. I. Alonso, G. Armelles, M. Ilg, and K. Ploog, *Phys. Rev. B* **47**, 12945 (1993).
- <sup>7</sup> Y. E. Khalifi, P. Lefebvre, J. Allègre, B. Gil, H. Mathieu, and T. Fukunaga, *Solid State Commun.* **75**, 677 (1990).
- <sup>8</sup> P. Vogl, H. P. Hjalmarson, and J. D. Dow, *J. Phys. Chem. Solids* **44**, 365 (1983).
- <sup>9</sup> D. J. Chadi, *Phys. Rev. B* **16**, 790 (1977).
- <sup>10</sup> F. García-Moliner and V. R. Velasco, *Theory of Single and Multiple Interfaces* (World Scientific, Singapore, 1992).
- <sup>11</sup> M. C. Muñoz, V. R. Velasco, and F. García-Moliner, *Phys. Rev. B* **39**, 1786 (1989).
- <sup>12</sup> G. Armelles, M. C. Muñoz, V. R. Velasco, and F. García-Moliner, *Superlatt. Microstruct.* **7**, 23 (1990).
- <sup>13</sup> D. A. Contreras-Solorio, V. R. Velasco, and F. García-Moliner, *Phys. Rev. B*, **47**, 4651 (1993); **48**, 12319 (1993).
- <sup>14</sup> W. I. Wang, T. S. Kuan, E. E. Mendez, and L. Esaki, *Phys. Rev. B* **31**, 6890 (1985).
- <sup>15</sup> A. Muñoz, J. Sánchez-Dehesa, and F. Flores, *Europhys. Lett.* **2**, 385 (1986); *Phys. Rev. B* **35**, 6468 (1987).
- <sup>16</sup> G. Platero, J. Sánchez-Dehesa, C. Tejedor, and F. Flores, *Surf. Sci.* **168**, 553 (1986).
- <sup>17</sup> *Landolt-Börnstein Numerical Data and Functional Relationships in Science and Technology*, Group III, Vol. 17a-b (Springer-Verlag, Berlin, 1982).
- <sup>18</sup> Yia-Chung Chang and D. E. Aspnes, *Phys. Rev. B* **41**, 12002 (1990).